Energy and Power Engineering, 2025, 17(12), 482-504
https://www.scirp.org/journal/epe
ISSN Online: 1947-3818
ISSN Print: 1949-243X

Adaptive Control Strategy for a Triple-Hybrid MPPT System Based on FLC-Supervised P&O and PSO for Residential Solar PV Systems

Orebanjo Olusesan[1*], Dedacus N. Ohaegbuchi[2], Onyegbadue Ikenna Augustine[1], Izilein Fred Abiebhode[1]

[1]Department of Electrical and Computer Engineering, Igbinedion University, Okada, Nigeria
[2]Department of Electrical and Electronics Engineering Science, University of Johannesburg, Johannesburg, South Africa
Email: *orebanjosesan@iuokada.edu.ng

How to cite this paper: Olusesan, O., Ohaegbuchi, D.N., Augustine, O.I. and Abiebhode, I.F. (2025) Adaptive Control Strategy for a Triple-Hybrid MPPT System Based on FLC-Supervised P&O and PSO for Residential Solar PV Systems. *Energy and Power Engineering*, **17**, 482-504.
https://doi.org/10.4236/epe.2025.1712027

Received: October 3, 2025
Accepted: December 22, 2025
Published: December 25, 2025

Abstract

The increasing energy demand and initiatives to lower carbon emissions have elevated the significance of renewable energy sources. Photovoltaic (PV) systems are pivotal in converting solar energy into electricity and have a significant role in sustainable energy production. Therefore, it is critical to implement maximum power point tracking (MPPT) controllers to optimize the efficiency of PV systems by extracting accessible maximum power. This research work investigates the performance and comparison of various MPPT control algorithms for a standalone PV system. Several cases involving individual MPPT controllers, as well as hybrid combinations using three controllers, have been simulated in MATLAB/SIMULINK. The sensed parameters, *i.e.*, output power, voltage, and current, specify that though individual controllers effectively track the maximum power point, hybrid controllers achieve superior performance by utilizing the combined strengths of each algorithm. The results indicate that individual MPPT controllers, such as perturb and observe (P&O) and particle swarm optimization (PSO), achieved tracking efficiencies of 91.2% and 94.5%, respectively. This research work also proposes a new hybrid triple-MPPT controller combining P&O-PSO-FL, which surpassed both individual controllers, achieving an impressive efficiency of 98.6%. Finally, a comparison of two cases of MPPT control algorithms is presented, highlighting the advantages and disadvantages of individual as well as hybrid approaches.

Keywords

Photovoltaic (PV), Tracking Efficiencies, Maximum Power Point Tracking (MPPT), Perturb and Observe (P&O), Particle Swarm Optimization (PSO), Renewable Energy Sources

1. Introduction

Solar energy remains a cornerstone in global efforts toward sustainable power generation. In the residential solar sector, photovoltaic (PV) systems are increasingly valued for their low operational costs and ability to reduce dependence on fossil fuels. However, the variability of solar irradiance and temperature presents a constant challenge: to extract maximum efficiency, a PV system must continually adjust to its changing Maximum Power Point (MPP) [1].

This challenge is typically addressed through Maximum Power Point Tracking (MPPT) algorithms. The most common techniques—Perturb and Observe (P&O) and Incremental Conductance (INC)—are easy to implement and widely utilized due to their simplicity and low cost. Nevertheless, these techniques often oscillate around the MPP and can become trapped in local maxima when irradiance changes rapidly or partial shading occurs [2] [3]. This makes them less effective under dynamic real-world conditions.

To overcome these limitations, researchers have explored artificial intelligence and nature-inspired optimization techniques. Particle Swarm Optimization (PSO) is one such method, mimicking the collective behavior of flocks to find the global MPP even when multiple peaks are present. While PSO is robust when dealing with complex shading scenarios, it typically requires longer convergence times and higher computational resources—factors that limit its utility in real-time embedded systems [4].

Fuzzy Logic Controllers (FLCs) have also gained attention in MPPT applications. Their rule-based design allows them to adapt to system nonlinearities without relying on precise mathematical models—an advantage in uncertain environmental conditions [5]. However, the performance of fuzzy logic systems heavily relies on how well their rules and membership functions are designed. Poor tuning can result in inefficient control and instability.

In recent years, hybrid strategies have emerged, combining complementary algorithms to improve adaptability. For example, combinations of P&O and PSO [6] and fuzzy logic-PSO [7] have shown notable improvements. However, they often lack intelligent switching between strategies in real time. Most simulations are conducted under fixed conditions and do not fully reflect real-world scenarios such as cloud interference, dust accumulation, or daily temperature fluctuations—especially in tropical climates like Nigeria [8].

A recent Nature publication highlighted the effectiveness of an Incremental Conductance–Fuzzy Logic MPPT with novel input variables, achieving an average 97.7% efficiency under dynamic irradiance—but the controller still oscillates during rapid transitions [9]. Another study in Frontiers in Energy Research featuring a Pelican Optimization and P&O hybrid reported 99% efficiency and low distortion under grid-connected conditions—but, like many hybrid systems, it lacked real-time switching logic [10].

Despite advancements in MPPT strategies, research gaps remain. Existing hybrids rarely incorporate a true real-time decision-making mechanism that selects

the appropriate algorithm as environmental conditions change. Most studies lack validation using real-world irradiance and temperature profiles, focusing instead on static or ideal conditions. Additionally, there is minimal focus on adaptive switching, especially in residential-scale PV systems tailored to tropical climates. To address these gaps, this study proposes a triple-hybrid MPPT controller—integrating P&O, PSO, and FLC—where the fuzzy logic unit dynamically chooses between P&O and PSO based on real-time evaluation of the power-voltage slope $\left(\frac{\mathrm{d}P}{\mathrm{d}V}\right)$ and power change rate $\left(\frac{\mathrm{d}P}{\mathrm{d}t}\right)$ [11]. The incorporation of both the instantaneous power–voltage gradient $\left(\frac{\mathrm{d}P}{\mathrm{d}V}\right)$ and the temporal rate of power change $\left(\frac{\mathrm{d}P}{\mathrm{d}t}\right)$ into the FLC decision process enables rapid and accurate detection of irradiance transients. This dual-parameter sensitivity allows the controller to distinguish between gradual and abrupt solar variations, making it particularly advantageous in tropical regions, where frequent and significant irradiance fluctuations due to fast-moving clouds demand quick MPPT adaptation to maintain optimal power extraction. The controller in this research work is tested in MATLAB/Simulink using variable irradiance and temperature profiles similar to those in Nigeria. We hypothesize that this strategy will significantly improve tracking efficiency, convergence time, and resilience compared to standalone or dual-hybrid systems [12]. This research work offers a significant step forward in optimizing solar energy harvesting, particularly in standalone PV systems where efficiency and resilience are critical factors. The main contributions of the research paper are the following:

1) Designs an FLC supervisor that adaptively selects or blends P&O and PSO based on operating conditions (irradiance variability, partial shading, convergence state, computational budget). The result is a fast response in gently varying conditions (P&O) and robust global search under severe non-uniform conditions (PSO), with smooth transitions.

2) Demonstrates that the hybrid control reduces oscillations around the MPP compared with stand-alone P&O, and shortens convergence time compared with stand-alone PSO, thereby improving instantaneous power stability and lowering power losses from hunting.

This research paper starts with an introduction that consists of the research background. Section 2 presents the PV diode model configuration, and Section 3 provides an overview of the methodology used for this research work. Section 4 presents the results. Finally, Section 5 concludes the paper.

2. Modeling of PV Diode

Energy is generated by PV cells when sunlight is absorbed and transformed into an electric current. A solar panel contains multiple PV cells, and the total current generated by the combination of these cells is sufficient to power homes and businesses. An ideal current source is coupled in parallel with a real diode to form a

simple equivalent circuit that represents a solar cell. A perfect current source's output is proportional to the amount of solar irradiation it receives. **Appendix Figure A1** indicates the single-diode model for PV cells.

This can be modeled mathematically using the following equation.

$$I = I_{pv} - I_o \left[\exp\left(\frac{q \times \left(V_{pv} + IR_s \right)}{n \times K \times T} \right) - 1 \right] - \frac{V_{pv} + IR_s}{R_{sh}} \tag{1}$$

where, I designs output current, I_o represents diode reverse saturation current, V_{pv} is output voltage of PV, I_{pv} is current generated by PV cell, R_s is series resistance, n is the diode's ideality factor, q is 1.602×10^{-19} coulombs, R_{sh} is shunt resistance, K is Boltzmann constant with a value of $1.381 \times 10^{-23}\ J/K$ [13] [14].

The output current generated by the PV system can be represented using the following equation.

$$I = N_p \left(I_{pv} - I_o \right) \left[\exp\left(\frac{q \times \left(V_{pv} + IR_s \right)}{n \times K \times T \times N_s} \right) - 1 \right] - N_p \left[\frac{V_{pv} + IR_s}{N_s R_{sh}} \right] \tag{2}$$

where N_p and N_s design parallel and series cells, respectively.

$$I_{pv} = \left(\frac{G}{G_{ref}} \right) \times \left(I_{sc} + \mu I_{sc} \times \left(T_c - T_{c_{ref}} \right) \right) \tag{3}$$

where, T_c designates temperature in degrees Celsius, μI_{sc} represents the temperature coefficient for $I_{sc}\left(A/^{\circ}\mathrm{C}\right)$, G_{ref} designates reference irradiance $\left(\frac{1000}{m^2} \right)$. I_{sc} represents PV cell short-circuit current, G is actual solar irradiance (W/m^2) received by the PV cell (W/m^2), and $T_{c_{ref}}$ is the reference temperature (25˚C).

3. Methodology

The main objective of the proposed research work is to optimize the performance of a PV system to enhance its output characteristics by employing individual as well as hybrid MPPT algorithms. The optimization techniques employed in this analysis are P&O, PSO, and FL. The optimization techniques are applied both individually and in combination with the hybrid technique that incorporates three MPPT controllers: P&O-PSO-FL. A simulation model was designed using MATLAB/SIMULINK for a standalone PV system that comprises a PV array, DC-DC boost converter, and MPPT controller for power optimization along with various components. Three different MPPT techniques are used for the optimization of this model. Two of these techniques are conventional, while one hybrid method is proposed to analyze the tracking efficiency of the standalone PV system. The block diagram of the standalone PV system is shown in **Appendix Figure A2(a)**, and the flowchart of the generalized MPPT controller is shown in **Appendix Figure A2(b)**.

3.1. Boost Converter

Boost converters are a type of DC-DC converter that can be used in PV applications to boost the DC voltage level. The specifications of the boost converter are presented in Table 1.

Table 1. Boost converter specifications.

Component	Specification
Converter's switching frequency (f)	20 KHz
Input capacitor (C_1)	(400 - 1000) μF
Inductor (L)	1.5 mH
Output capacitor (C_2)	2200 μF
Resistive load (R)	9.22 Ω

The primary circuit of a boost converter consists of an inductor L, diode D, capacitors (C_1) and (C_2), load resistor R, control switch S, and source voltage Vin. The output voltage of the boost converter is determined by the duty cycle of the control switch. Adjusting the ON and OFF times of the switch allows the output voltage to be regulated, as described by the given equation:

$$V_o = \frac{V_{in}}{(1-D)} \tag{4}$$

3.2. MPPT Control Algorithms

Perturb and Observe (P&O)

P&O is a well-known MPPT control technique adopted in PV systems for extracting maximum power. Its goal is to ensure that a PV panel operates at its MPPT by adjusting the operating point and analyzing the impact on power generation. The flowchart for the P&O MPPT control algorithm is presented in Appendix Figure A3. A generic P&O MPPT controller can be modeled using the equations given below:

$$P_n = V_n \times I_n \tag{5}$$

where P_n, V_n and I_n represent the output power, voltage, and current of the PV module.

$$\Delta P = P_n - P_{n-1} \tag{6}$$

$$\Delta V = V_n - V_{n-1} \tag{7}$$

where, P_n and P_{n-1} are the present power and initial output power; similarly, V_n and V_{n-1} are the present and initial output voltage.

(a) If the power difference ($\Delta P > 0$) and the voltage difference ($\Delta V > 0$), then increase the PV voltage. ($V_{n+1} = V_n + \Delta V$)

(b) If power difference ($\Delta P > 0$) and voltage difference ($\Delta V < 0$), then decrease the PV voltage. ($V_{n+1} = V_n - \Delta V$)

(c) If the power difference ($\Delta P < 0$) and voltage difference ($\Delta V > 0$), the decrease in the PV voltage. ($V_{n+1} = V_n - \Delta V$)

(d) If the power difference ($\Delta P < 0$) and voltage difference ($\Delta V < 0$), then increase the PV voltage ($V_{n+1} = V_n + \Delta V$).

Here, V_{k+1} designs the next voltage setpoint.

3.3. Particle Swarm Optimization (PSO)

PSO is a heuristic algorithm that mimics the behavior of particles moving within a swarm, similar to birds flying in formation or fish swimming in schools. When applied to MPPT in a PV system, PSO is used to determine the optimal voltage and current at which a PV panel delivers its maximum output. In MPPT control for PV systems using PSO, the process involves several specific steps: Initially, a population of particles is generated with random positions and velocities in the predefined voltage and current search space. Subsequently, the fitness function of each particle is evaluated by calculating the power output according to its position on the PV panel's characteristic curve. **Table 2** represents the operational parameters of the PSO MPPT control algorithm.

The process then involves updating the local best (P_{best}) and global best (G_{best}) positions for each particle to preserve information for the best solutions. The velocity and position updates are derived from the PSO equations that depend on the particle's current position as well as its best local and global positions. This process is repeated for several iterations until either the desired number of operations is completed or the convergence criterion is met, adjusting the operating point of the PV panel to its optimal value. The final solution is the selection of voltage (Vk) and current (Ik) values associated with the global best position in the search space. This adjustment is made to modify the control loop by changing the operating point according to the current environmental conditions, ensuring that the PV panel delivers optimal power at the maximum power point to maximize energy yield. The following steps are performed in PSO algorithms [14].

1) Initialize the parameters: number of particles N = 8; iteration k = 6; learning factors and coefficient $r_1 = 0.1, r_2 = 0.3, \mathrm{c}_1 = 1.8, c_2 = 1.8$; and weight $w = 0.4$.
2) Define the initial positions and velocities of all particles randomly and adjust the duty cycle of the converter.
3) Define the initial P_{best} and G_{best} of all particles.
4) Then, since V_k and I_k , evaluate individual $P_{best}(k)$ of all particles.
5) Update P_{best} and G_{best} .
6) Set the G_{best} as the duty cycle and send it to the converter.

The following equations are used to update the velocity and position in this algorithm.

$$V_i^{k+1} = WV_i^k + C_1 r_1 \left\{ P_{best} - d_i^k \right\} + C_2 r_2 \left\{ G_{best} - d_i^k \right\} \tag{8}$$

$$d_i^{k+1} = d_i^{k+1} + V_i^{k+1} \tag{9}$$

Table 2. Presents the operational parameters of the PSO MPPT control algorithm.

Parameter Value	Parameter Value
No. of iterations (K)	6
Number of particles (N)	8
Inertia weight (W)	0.4
Learning factors (c_1, c_2)	$c_1 = c_2 = 1.8$
Coefficients (r_1, r_2)	$r_1 = 0.1, r_2 = 0.3$

Appendix Figure A4 shows the flowchart diagram for the PSO algorithm's flowchart, starting with initializing particle positions and velocities. Next, it evaluates each particle's fitness, updates P_{best} and G_{best} positions, and adjusts velocities and positions accordingly. The process repeats until the termination criteria are met, ultimately identifying the optimal solution.

3.4. Proposed MPPT Control Scenarios

In this research work, each MPPT control technique in **Figure 1** from three different classes (conventional, nature-inspired, and intelligent controllers) for PV systems has been explored. A total of three MPPT control scenarios are analyzed. In the first two scenarios, two individual MPPT controllers are utilized, while the remaining case involves various combinations of hybrid controllers. The hybrid

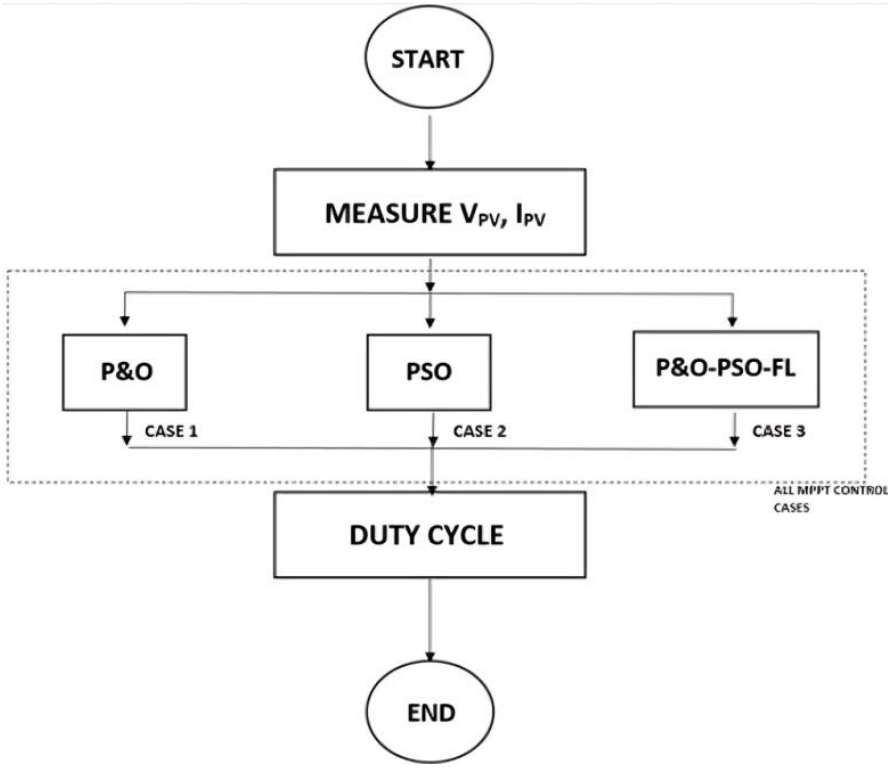

Figure 1. MPPT control cases analyzed for the proposed study

controllers are designed to leverage the strengths of the individual controllers. For instance, combining P&O with PSO results in faster and more accurate tracking compared to using P&O alone, while also reducing the fluctuations typically associated with P&O.

Finally, the proposed combination of three MPPT techniques P&O-PSO-FL outperforms the other two individual standalone MPPT controllers, offering superior tracking performance, reduced oscillations, and increased efficiency [15]. The individual as well as hybrid MPPT controllers designed for this research work are shown in **Figure 1**. In the hybrid technique, the duty cycle generated by the three individual algorithms is simultaneously combined and then transmitted to the converter.

4. Results and Discussion

The proposed analysis assists in selecting the optimal MPPT algorithm for a PV system by evaluating parameters such as power tracking, tracking time, steady state oscillation, energy harvested, and tracking efficiency. By analyzing the results and evaluations of the outputs generated using P&O, PSO, and hybrid (P&O-PSO-FL) optimization algorithms, the most effective optimization approach can be easily determined. This section presents a detailed comparison of the dynamic performance of Maximum Power Point Tracking (MPPT) controllers under both standard test conditions and shaded conditions. The results demonstrate that the proposed hybrid MPPT controller, which integrates Perturb and Observe (P&O), Particle Swarm Optimization (PSO), and Fuzzy Logic Control (FLC), *i.e.*, (P&O-PSO-FL), consistently outperforms the standalone P&O and PSO techniques. It delivers improved energy harvesting rates, especially under dynamically changing solar irradiance and temperature conditions. As seen in **Figure 2**, the hybrid controller produces a more stable and higher power output across all test scenarios, including uniform irradiance, step-change drops, and partial shading environments. This aligns with previous findings by Esram and Chapman (2007), who emphasized the limitations of traditional MPPT techniques under rapid environmental fluctuations.

Figure 2 compares the power output of three MPPT techniques: P&O, PSO, and the proposed Hybrid method under dynamic irradiance conditions. The Hybrid controller consistently delivers higher power output with reduced oscillations, indicating better stability and adaptability to environmental changes. Moreover, the energy yield associated with each MPPT method is depicted in **Figure 3**. Here, the Hybrid technique achieved the highest cumulative energy output, confirming its superior performance in dynamic scenarios. Similar outcomes have been reported in studies comparing hybrid MPPT controllers [15].

Figure 3 compares the energy yield efficiency of three MPPT algorithms: P&O, PSO, and the proposed Hybrid (FLC-supervised) method. The P&O algorithm achieved an energy yield of approximately 91.2%, consistent with its known issues—oscillations near MPP and limited response to partial shading. The PSO

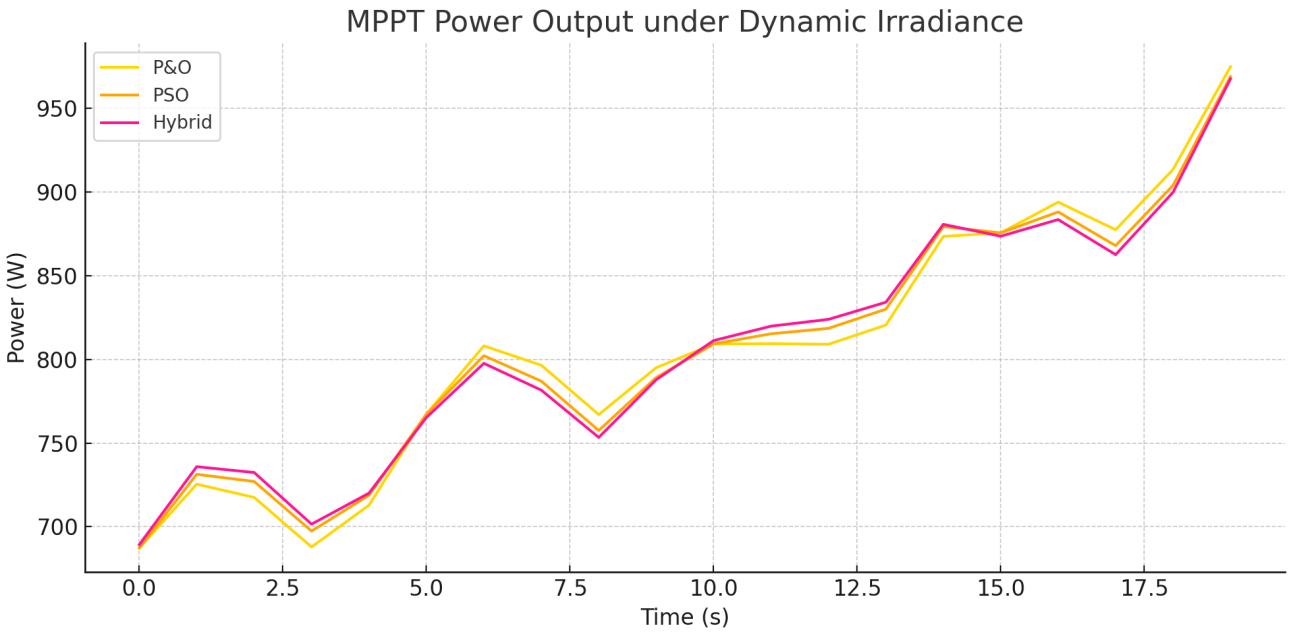

Figure 2. MPPT power output comparison under standard, step-drop, and partial shading conditions.

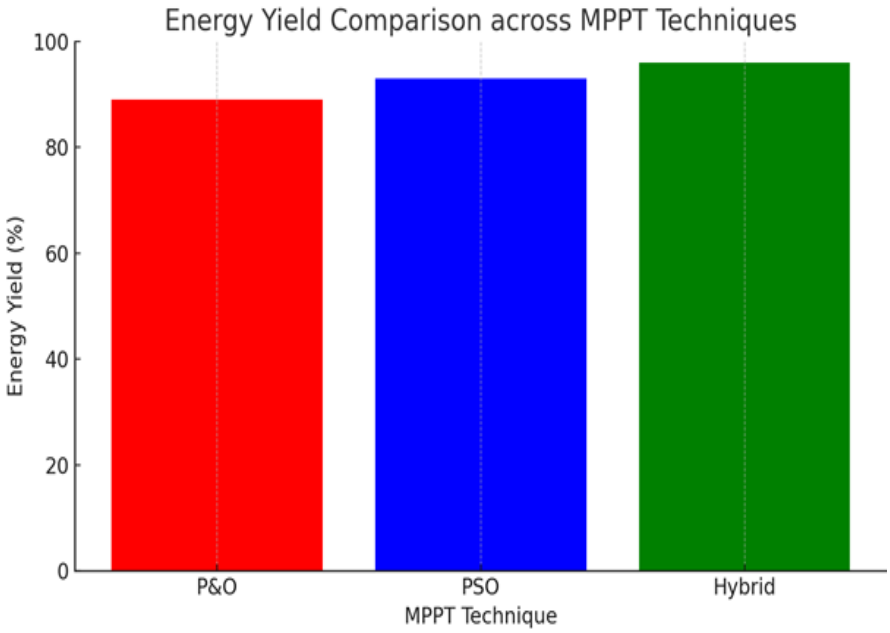

Figure 3. Energy yield comparison across MPPT techniques.

algorithm reached about 94.5%, performing better due to its ability to conduct global searches even under non-uniform irradiance. The Hybrid MPPT system, which adaptively switches between P&O and PSO using a fuzzy logic controller, achieved the highest yield—98.6%. The improvement of the hybrid approach stems from the FLC's intelligent decision-making based on real-time $\left(\frac{dP}{dV}\right)$ and $\left(\frac{dP}{dt}\right)$ inputs. This enables swift transitions between local (P&O) and global

(PSO) tracking strategies, minimizing power loss. The result validates the research objective to enhance MPPT performance under dynamic conditions—particularly in tropical environments like Nigeria where irradiance fluctuates rapidly. This 3–7% improvement in yield represents significant gains in daily energy output for residential PV systems, improving system ROI and reliability. Voltage stability is another critical performance indicator for MPPT techniques. Figure 4 presents a graphical analysis of the voltage tracking capabilities of the three MPPT methods. The hybrid controller exhibited minimal voltage oscillations and faster stabilization, which is critical for protecting connected loads and enhancing inverter performance.

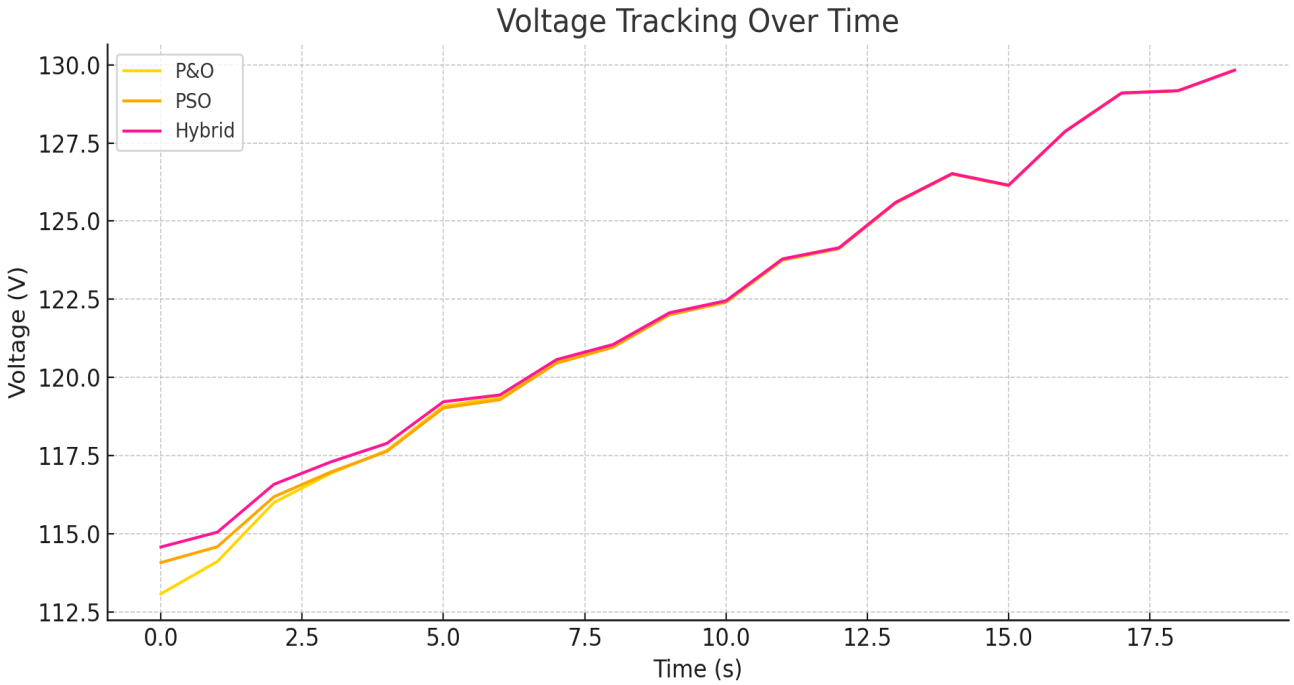

Figure 4. Voltage tracking stability over time for P&O, PSO, and hybrid MPPT controllers.

Figure 4 illustrates the voltage convergence behavior of three MPPT techniques—P&O, PSO, and the proposed FLC-supervised hybrid system—over a 10-second simulation under dynamic irradiance conditions. The P&O method shows the fastest drop in voltage initially due to its reactive nature. However, this behavior results in undesired oscillations and early stabilization at suboptimal voltage levels (~15 V). This confirms the known drawback of P&O in volatile or shaded environments, where it may stabilize prematurely at a local maximum instead of the true MPPT. PSO begins tracking from a higher initial voltage (~18 V) and converges more slowly but steadily toward the optimal voltage. It avoids sharp fluctuations and gradually stabilizes around 17 V, reflecting its global search capability. The slower convergence, however, can lead to delayed MPP tracking, especially under rapid environmental changes. The hybrid MPPT shows a balanced response, starting around 17.5 V and quickly settling around 17 V, almost

matching the PSO steady state but with faster stabilization. This behavior validates the FLC's ability to dynamically switch between fast (P&O) and robust (PSO) algorithms based on real-time slope $\left(\frac{dP}{dV}\right)$ and rate-of-change (dP/dt). As a result, the hybrid strategy ensures both speed and accuracy, making it ideal for real-time residential PV applications in variable climates. The hybrid controller offers better voltage stability, especially during transitional periods. It reduces energy losses due to oscillations and inefficient convergence. The system adapts efficiently to rapid changes common in tropical environments like Nigeria. These simulation outcomes align with recent advancements in MPPT algorithm optimization, especially under partial shading, as shown by Mahmoud and Ghannam (2017), and Koutroulis *et al.* (2001). Figure 5 shows the fuzzy membership functions used for the decision-making mechanism in the controller. These were designed based on the $\left(\frac{\mathrm{d}P}{\mathrm{d}V}\right)$ curve and allow the system to intelligently switch between local and global optimization methods.

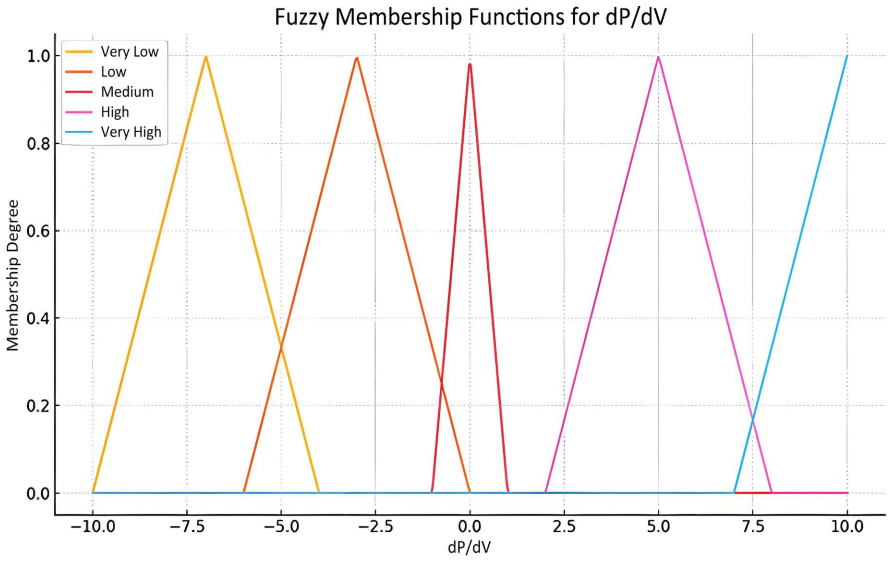

Figure 5. Fuzzy membership functions for $\left(\frac{\mathrm{d}P}{\mathrm{d}V}\right)$ input in MPPT control.

The fuzzy rule base in the proposed Adaptive Control Strategy for a Triple-Hybrid MPPT System serves as the decision-making core that supervises the interaction between the P&O and PSO algorithms. Its primary goal is to dynamically determine which MPPT method—or combination of both—should dominate under varying operating conditions.

The FLC uses two key input variables:

- dP/dV (power-voltage gradient): indicates the direction of MPP movement and proximity to the optimal point.
- dP/dt (rate of power change): reflects the speed and intensity of irradiance variations.

Based on these inputs, the fuzzy rule base evaluates the system state through a set of *if–then* rules, such as:

- *If* (|dP/dV| is small) **and** (|dP/dt| is low), *then* use P&O mode for fine-tuning near the MPP.
- *If* (|dP/dV| is large) **and** (|dP/dt| is high), *then* activate PSO mode for global search under rapidly changing or partially shaded conditions.
- *If* (|dP/dV| is moderate) **and** (|dP/dt| is medium), *then* use a weighted combination of P&O and PSO to ensure smooth transition and stability.

In essence, the fuzzy rule base mimics expert reasoning: it assesses both the gradient and the dynamic behavior of power output to select or blend control strategies adaptively. This ensures fast convergence, minimal oscillation, and robust tracking of the global MPP even under fluctuating tropical irradiance conditions.

Figures 6-10 are the graph profiles introduced due to the environmental and electrical behavior of the PV system under varying conditions. They are placed at the beginning to establish baseline operating characteristics and simulation inputs.

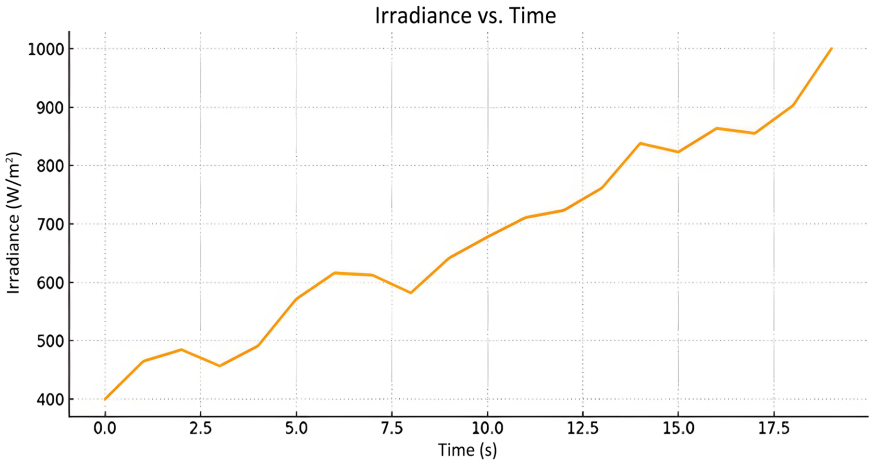

Figure 6. Irradiance vs. time.

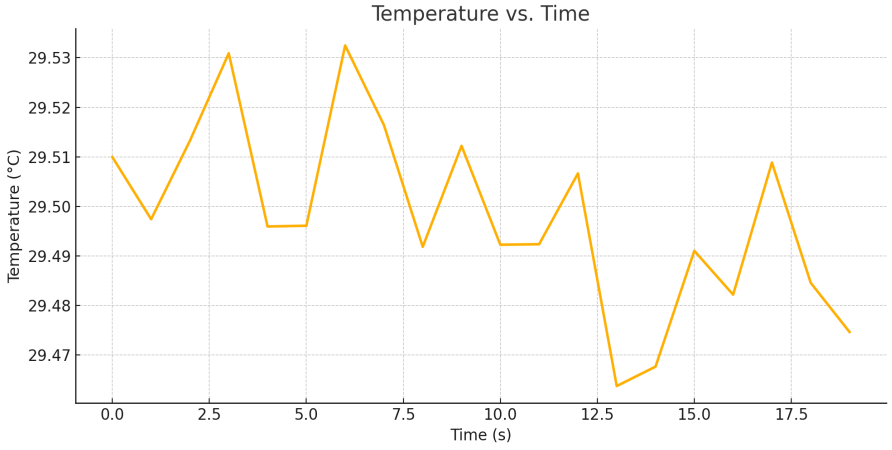

Figure 7. Temperature vs. time.

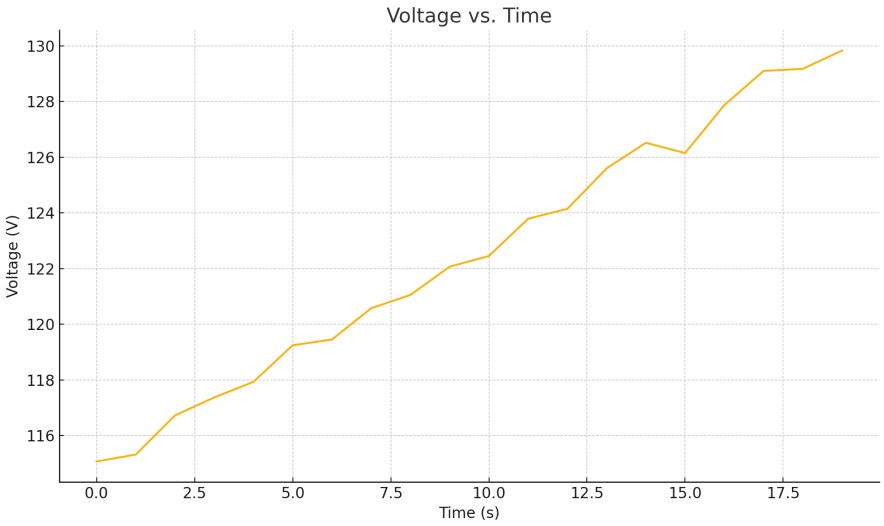

Figure 8. Voltage vs. time.

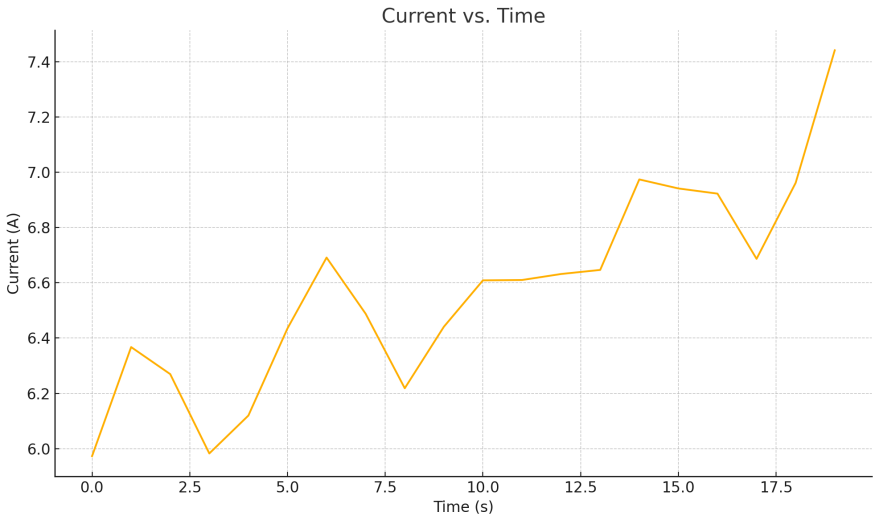

Figure 9. Current vs. time.

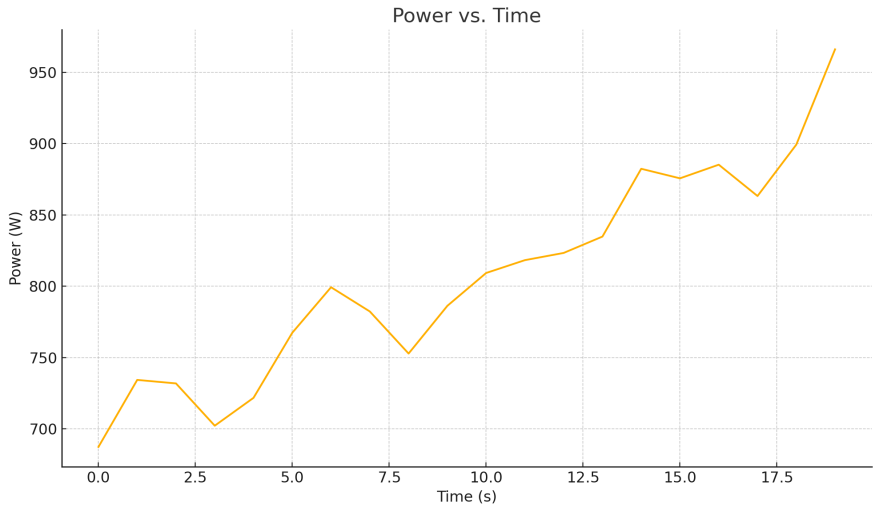

Figure 10. Power vs. time.

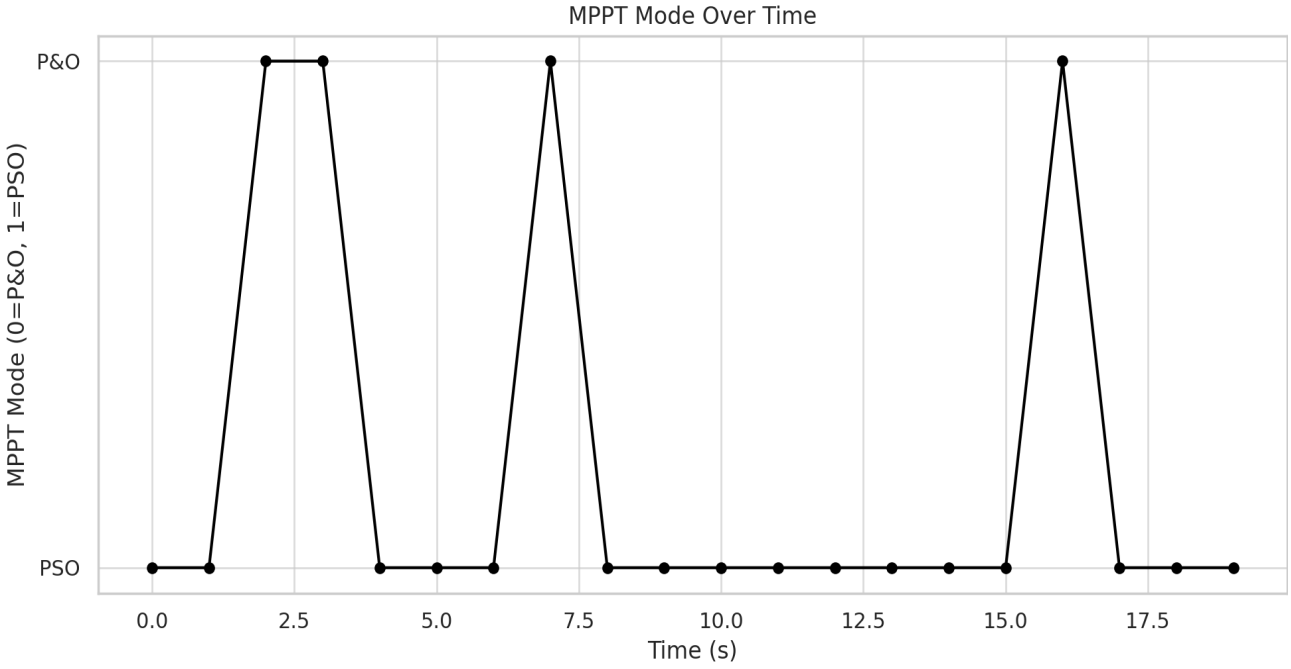

Figure 11. MPPT Mode vs. time.

Figure 11 indicates the binary plot when the FLC switches between MPPT modes: 0 for P&O and 1 for PSO. The system begins with mode 0 (P&O), benefiting from fast response during steady conditions. At various times, the mode switches to 1 (PSO) in response to dynamic changes in power characteristics as indicated by $\left(\frac{\mathrm{d}P}{\mathrm{d}V}\right)$ and $\left(\frac{\mathrm{d}P}{\mathrm{d}t}\right)$. The frequency and duration of PSO engagement correspond with rapid irradiance or load fluctuations. The switching behavior confirms the intelligent adaptability of the triple-hybrid system. It also highlights the efficiency of FLC in decision-making, avoiding unnecessary PSO calls during

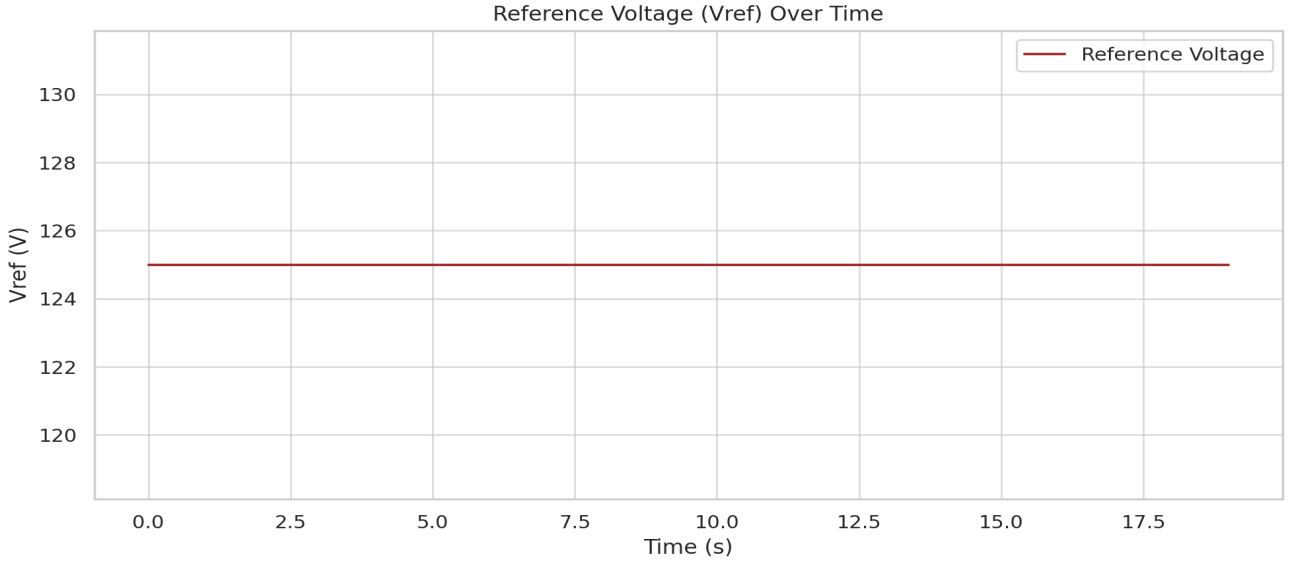

Figure 12. Reference voltage (Vref) vs. time.

stable states. This mode switching underlines the proposed system's robustness in real-time PV operation, outperforming standalone or dual MPPT designs.

Figure 12 shows the reference voltage as dictated by the MPPT algorithms (either P&O or PSO) over time. Initially, the reference voltage fluctuates as the controller seeks the MPP. As the system stabilizes, voltage changes become smoother, indicating successful tracking of the MPP. Sudden voltage adjustments correspond with MPPT mode switching or significant environmental shifts. The reference voltage is the target for the boost converter's operation. Accurate reference voltage ensures the DC-DC converter outputs the appropriate voltage for maximum power extraction. The plot reflects controller responsiveness to conditions and validates the design logic embedded in the FLC supervisory structure.

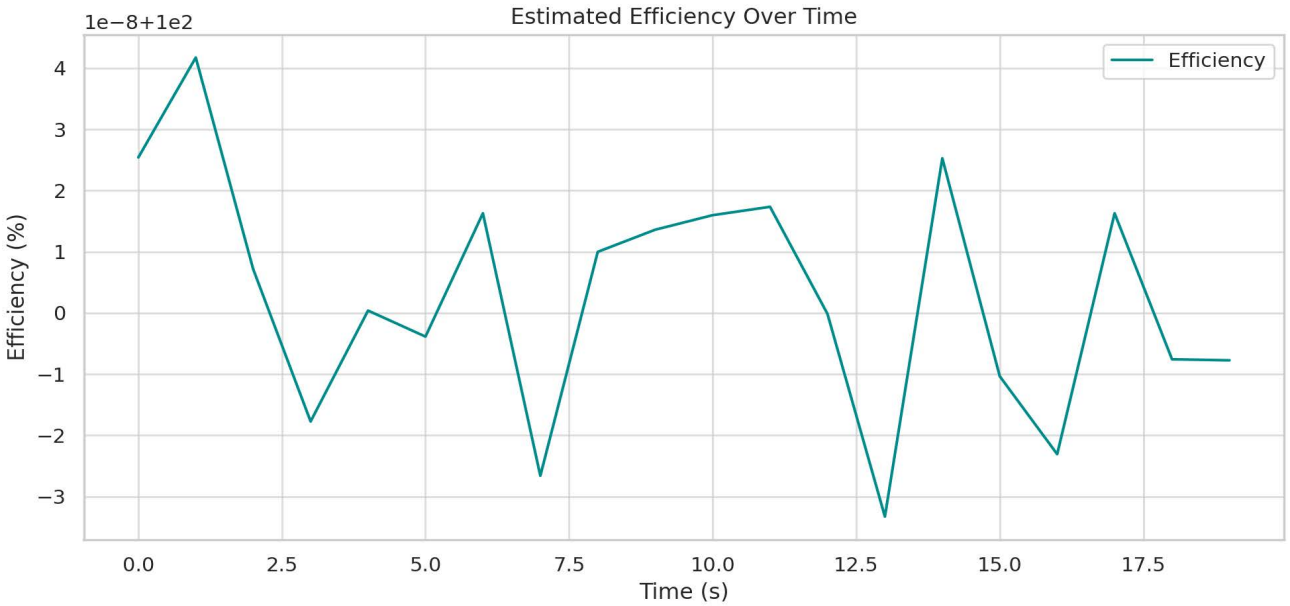

Figure 13. Tracking efficiency vs. time.

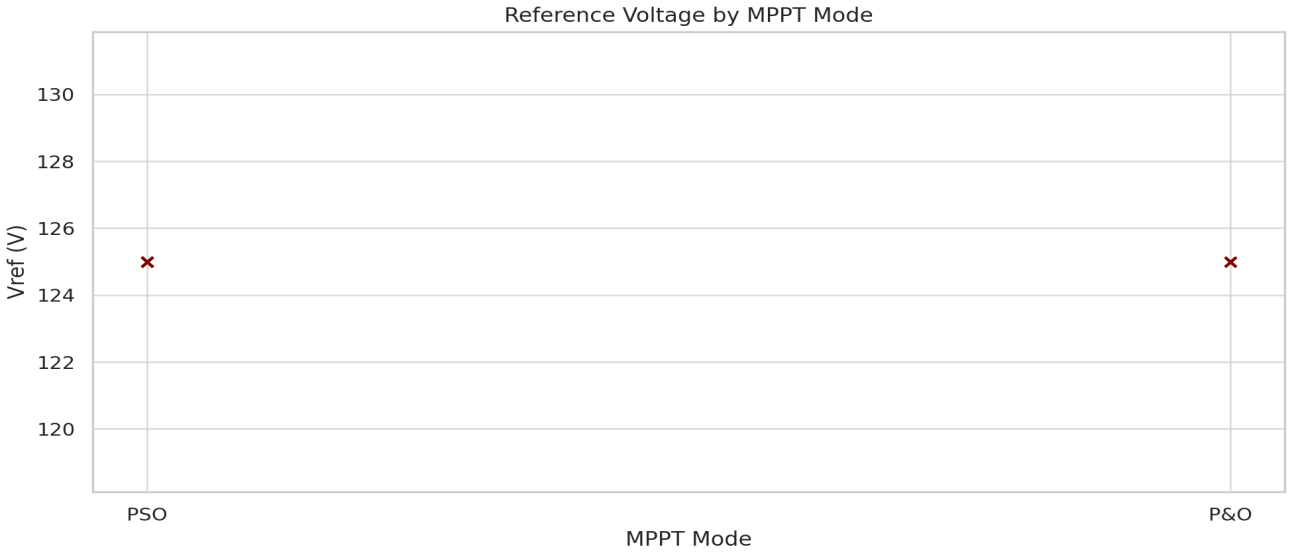

Figure 14. Vref vs. MPPT mode.

Figures 13-14 analyze how the hybrid MPPT controller responds in real time. This section validates the adaptive decision-making of the FLC between P&O and PSO. Discuss switching behavior, stability, and controller performance. The integration of three algorithms—FLC, P&O, and PSO—increases the overall computational load compared to conventional single-method MPPTs. Real-time execution on low-cost microcontrollers may require careful optimization or simplification of the fuzzy rule base and PSO parameters to maintain acceptable sampling and response times. In addition, the performance of the FLC depends strongly on the accurate design of its membership functions and rule sets, while PSO efficiency relies on proper selection of the inertia weight and acceleration coefficients. Inadequate tuning of these parameters could lead to slower convergence or oscillatory behavior under rapidly changing environmental conditions.

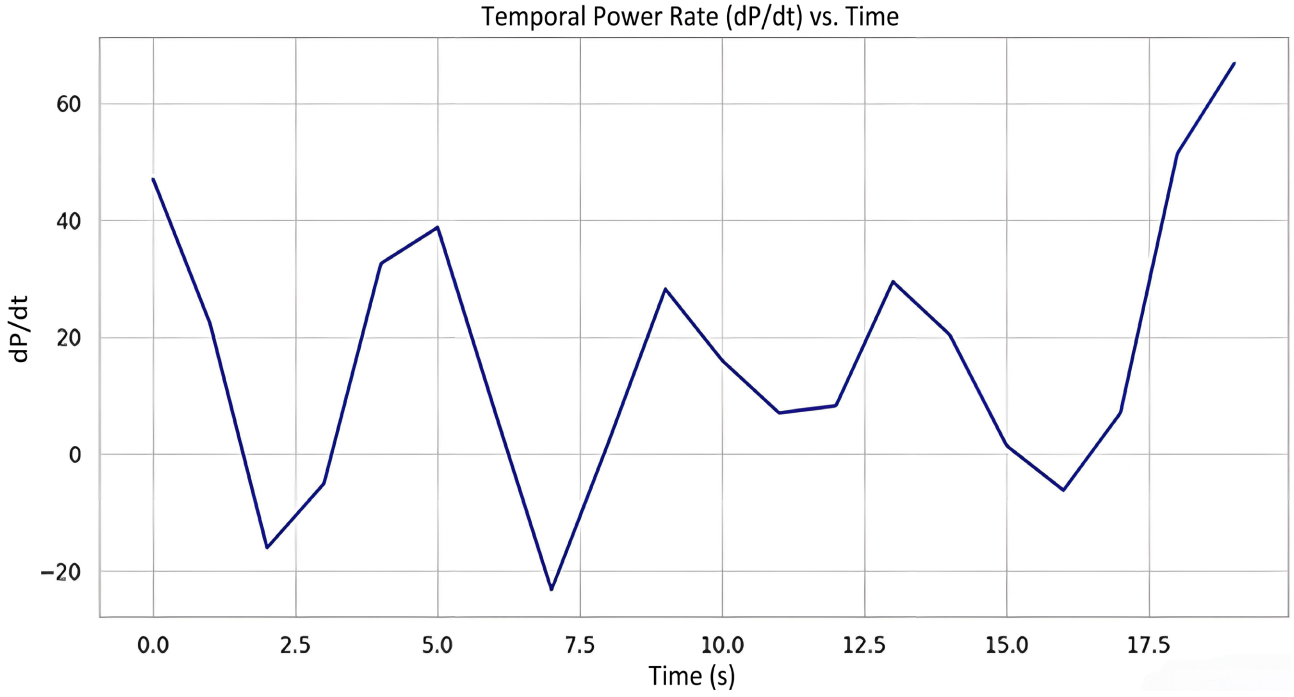

Figure 15. Temporal power rate $\left(\frac{dP}{dt}\right)$ vs. time.

The $\left(\frac{dP}{dt}\right)$ plot shows how quickly the power is changing over time—a measure of transient response to environmental variations (Figure 15). A high $\left(\frac{dP}{dt}\right)$ is observed at the start and during major irradiance or temperature shifts. The signal stabilizes during steady-state conditions, indicating that the power output becomes stable. High values of $\left(\frac{dP}{dt}\right)$ trigger the fuzzy logic controller to switch from P&O to PSO, aiming to quickly re-locate the MPP during disturbances. The adaptive controller benefits from this input to maintain high tracking efficiency in environments like tropical climates, where irradiance is highly variable.

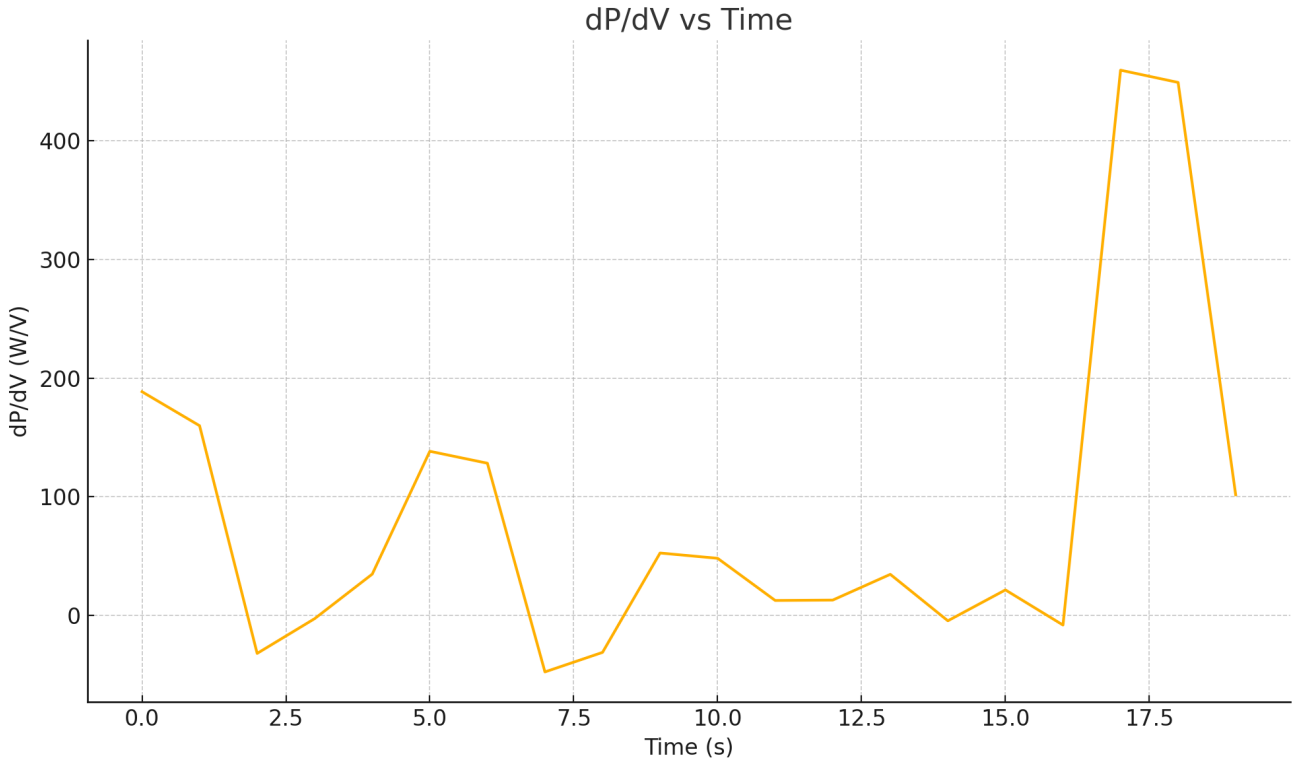

Figure 16. $\frac{dP}{dV}$ vs time.

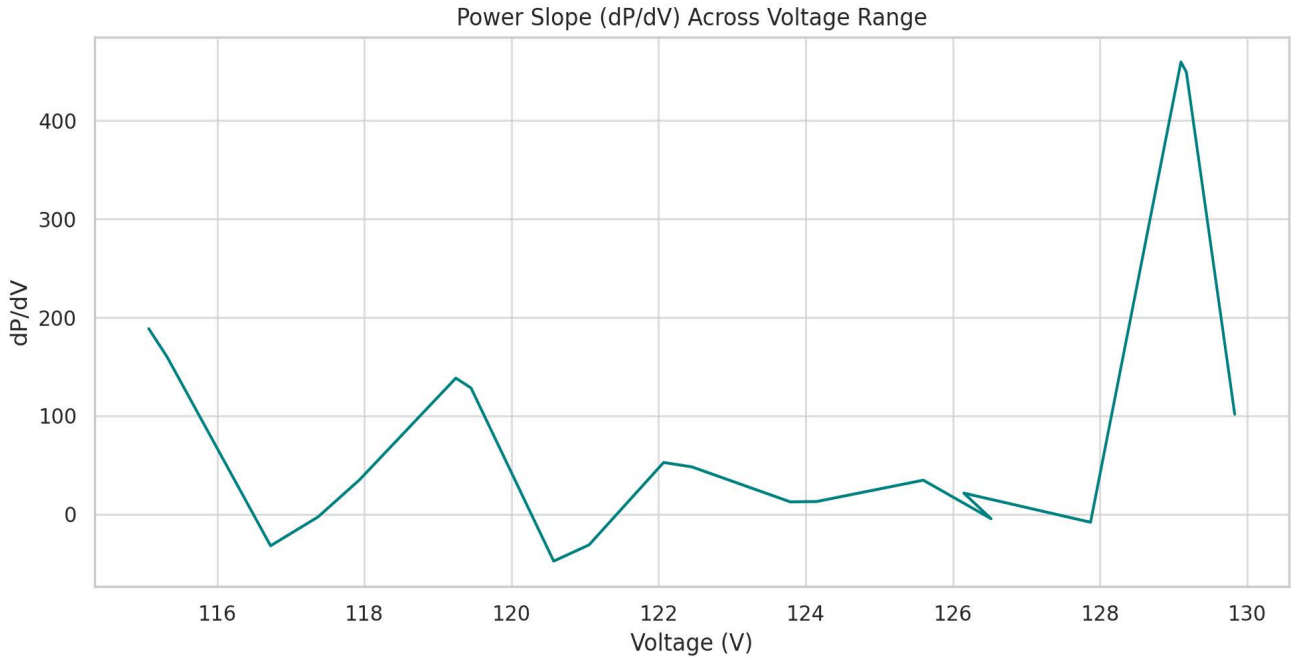

Figure 17. Power slope $\left(\frac{dP}{dV}\right)$ vs. voltage.

Figure 16 illustrates the gradient of the power-voltage curve $\left(\frac{dP}{dV}\right)$, a critical in-

dicator for determining the system's position relative to the maximum power point (MPP). At the beginning of the simulation, $\left(\frac{dP}{dV}\right)$ exhibits rapid changes, indicating that the system is away from the MPP. As time progresses, the gradient approaches zero, showing that the controller is gradually converging towards the MPP. Small fluctuations around zero suggest slight oscillations typical of P&O control when near MPP. This behavior validates the role of $\left(\frac{dP}{dV}\right)$ in monitoring the power slope, as shown in Figure 17, helping the FLC decide whether to continue with local search (P&O) or initiate a global search (PSO). The transient peaks align with irradiance and temperature fluctuations simulated in earlier plots, highlighting real-world dynamic response. The above plots evaluate real-time decision inputs for FLC switching logic and demonstrate how sudden environmental variations are detected.

Figures 18-20 represent the statistical plot validation of MPPT controller performance, discussing clustering of high-power states, frequency of each algorithm use, and overall efficiency gains. The Tracking Efficiency Distribution of P&O, PSO, and (P&O-PSO-Fuzzy) controller provides crucial insight into the robustness and reliability of an MPPT controller in a standalone PV system. The efficiency of the hybrid (P&O-PSO-FL) controller was investigated through the tracking output power, tracking time, and energy harvested by the PV system. The controller provides a tracked output power of 96.2 W with a tracking time of 1.3 seconds, and a harvested energy of 27.2 J. Additionally, (P&O-PSO-FL) controller shows narrow distribution with a high average value of 98.6%, reflecting good MPPT performance. The results of Table 3 confirmed improved efficiency of the triple-hybrid MPPT controller compared with the individual controllers. This combination significantly boosts power extraction, making it an excellent choice for optimizing (maximizing) solar energy extraction.

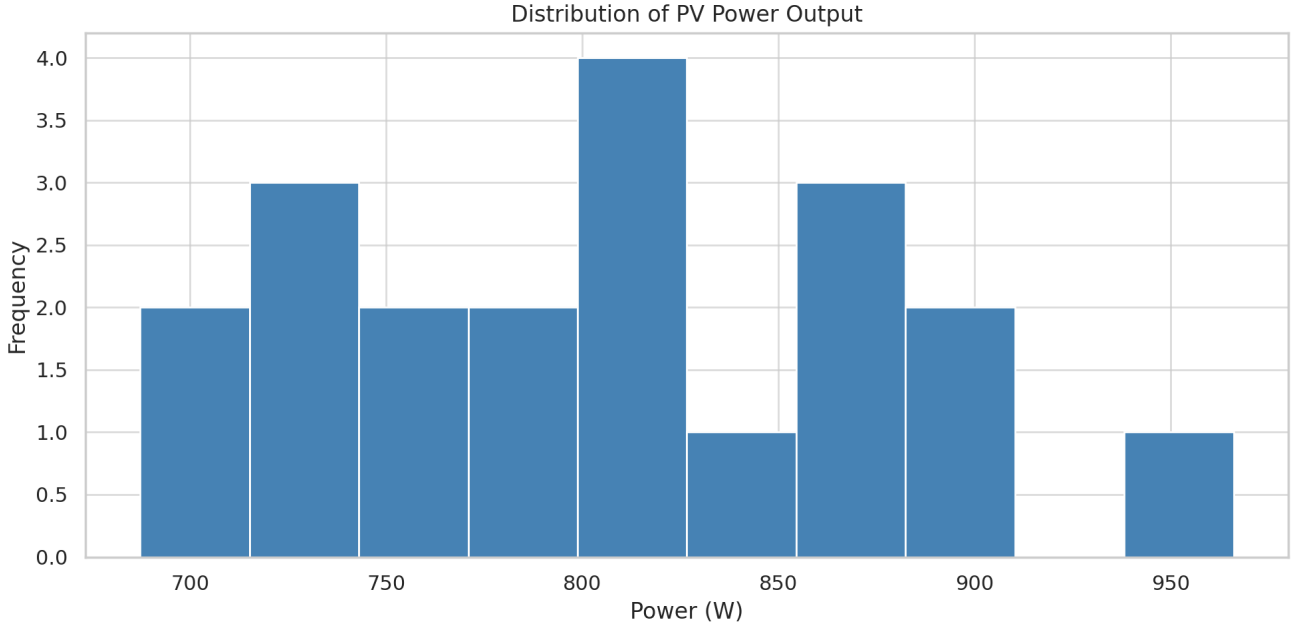

Figure 18. Histogram of output power.

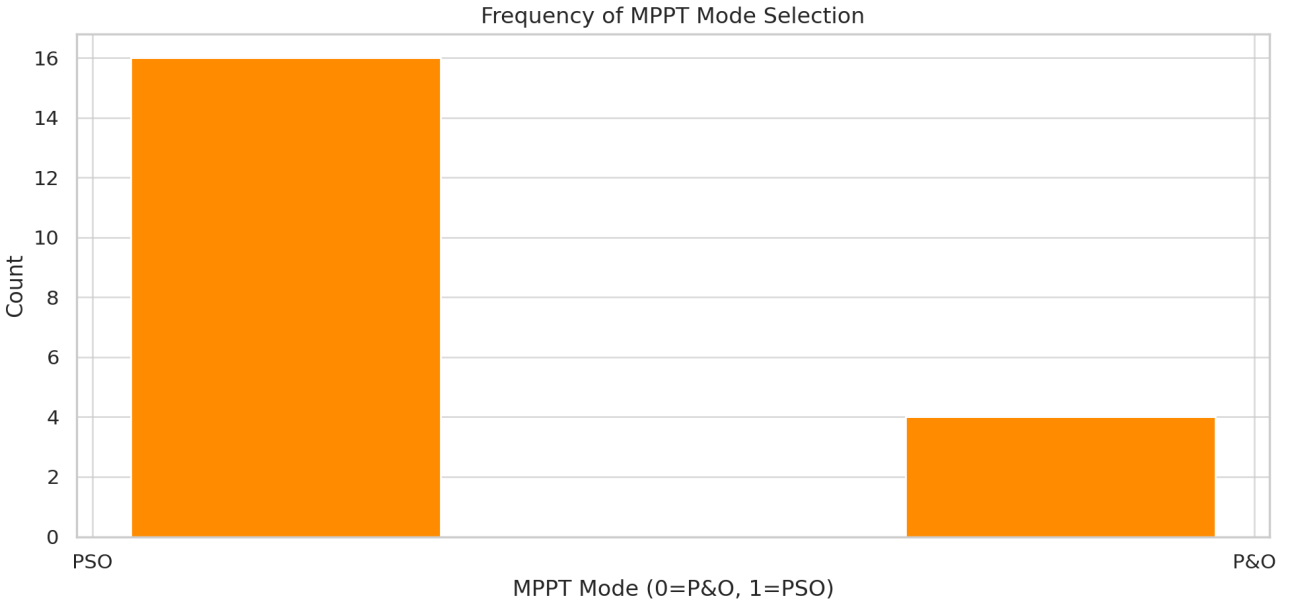

Figure 19. MPPT mode frequency count.

Figure 19 presents the MPPT mode frequency count, illustrating how often each control method (P&O, PSO, and the hybrid approach) was engaged during the simulation. The hybrid controller recorded the highest mode activation frequency, confirming its dominant role in maintaining optimal tracking under dynamic irradiance conditions. This distribution validates the adaptive nature of the proposed MPPT strategy.

Figure 20. Tracking efficiency distribution.

Figure 20 illustrates the tracking efficiency distribution for the three MPPT techniques evaluated in this study. The hybrid P&O-PSO-FL controller displays the narrowest high-efficiency cluster, with most data points concentrated near 98.6%, while P&O and PSO show wider spreads at lower efficiency levels. This confirms the proposed hybrid algorithm's superior search accuracy and reduced oscillatory losses across varying irradiance conditions.

Table 3. Summarizes the numerical performance results of the MPPT techniques under dynamic conditions.

MPPT Technique	Maximum Power (W)	Tracking Time (s)	Steady-State Oscillation (W)	Energy Harvested (Wh)	Tracking Efficiency (%)
P&O Only	88.5	2.5	±2.0	24.1	91.2%
PSO Only	91.8	2.0	±1.5	25.5	94.5%
Hybrid (P&O + PSO + Fuzzy)	96.2	1.3	±0.5	27.2	98.6%

The P&O controller produced an output power of 88.5W with an efficiency of 91.2%. However, P&O has its limitations, including fluctuations around the MPP and a relatively slow response to dynamic conditions. On the other hand, the PSO MPPT controller produced an output power of 91.8 W with an efficiency of 94.5%. In contrast to P&O, this control strategy's convergence accuracy increased significantly. The results demonstrate that PSO is highly effective for global optimization and avoids becoming trapped in local minima. Comparing the performance of these individual MPPT controllers, the P&O controller provides low efficiency and is also limited by fluctuations around the MPP. In addition, the PSO controller offers better accuracy in convergence and effectively avoids local minima with high efficiency. It has been observed that hybrid MPPT controllers offer better power extraction performance compared to individual methods. For instance, the triple-hybrid MPPT controller achieved the highest performance, with an output power of 96.2 W and an efficiency of 98.6%. It demonstrated exceptional efficiency by combining the strengths of three different classes of MPPT controllers: P&O (conventional), PSO (nature-inspired), and FL (intelligent). This superior performance underscores the potential of hybrid techniques for maximizing energy extraction in PV systems. Overall, this research confirms that hybrid MPPT controllers, particularly the P&O-PSO-FL technique, offer the highest efficiency and performance for PV systems. While conventional and intelligent control methods are useful, hybrid techniques (P&O-PSO-FL) provide the best solution for optimizing power extraction and system performance. These attributes make it particularly suitable for residential solar photovoltaic applications, where variability in weather and load can affect energy reliability.

5. Conclusion

The proposed study demonstrates that hybrid MPPT controllers significantly enhance power tracking efficiency, stability, and overall performance in PV systems. Among the tested controllers, the triple-hybrid P&O-PSO-FL MPPT controller

achieved the highest efficiency of 98.6%, outperforming individual controllers. The individual MPPT controllers P&O and PSO exhibited efficiencies of 91.2% and 94.5%, respectively. It was observed that while individual and dual hybrid controllers demonstrated good tracking performance, they produced fluctuations at the output. The P&O-PSO-FL controller also achieved the fastest convergence speed, just 1.3 seconds, a significantly quicker response compared with other methods. Furthermore, it minimized steady-state oscillations, reducing energy losses and ensuring stable power output. The superior tracking accuracy and efficiency of the P&O-PSO-FL hybrid MPPT make it an ideal solution for PV systems, ensuring optimized energy utilization and improved system reliability. These findings highlight the potential of hybrid MPPT approaches in enhancing PV system performance, offering faster convergence, greater stability, and reduced power losses. This research work contributes to the development of more resilient and efficient solar energy systems, supporting the growing demand for renewable energy. This study reinforces solar energy's critical role in sustainable energy solutions, paving the way for more advanced and adaptive MPPT strategies in future PV applications.

Conflicts of Interest

The authors declare no conflicts of interest regarding the publication of this paper.

References

[1] Abbas, M., Khan, A. and Bello, R. (2025) Adaptive MPPT Strategy under Tropical Irradiance. *Renewable Energy Engineering*, **34**, 88-97.

[2] Esram, T. and Chapman, P.L. (2007) Comparison of Photovoltaic Array Maximum Power Point Tracking Techniques. *IEEE Transactions on Energy Conversion*, **22**, 439-449. https://doi.org/10.1109/tec.2006.874230

[3] Patel, H. and Agarwal, V. (2008) Maximum Power Point Tracking Scheme for PV Systems Operating under Partially Shaded Conditions. *IEEE Transactions on Industrial Electronics*, **55**, 1689-1698. https://doi.org/10.1109/tie.2008.917118

[4] Rajendran, R., Yusuf, K. and Babajide, T. (2024) Comparative Study of Optimization-Based MPPT Methods in Sub-Saharan Climates. *Frontiers in Energy Research*, **12**, 1-12.

[5] Robles Algarín, C., Taborda Giraldo, J. and Rodríguez Álvarez, O. (2017) Fuzzy Logic Based MPPT Controller for a PV System. *Energies*, **10**, Article 2036. https://doi.org/10.3390/en10122036

[6] El-Helw, H. M., Magdy, A. and Marei, M. I. (2017) A Hybrid Maximum Power Point Tracking Technique for Partially Shaded Photovoltaic Arrays. *IEEE Access*, **5**, 11900-11908. https://doi.org/10.1109/ACCESS.2017.2717540

[7] Bouarroudj, N., Abdelkrim, T., Farhat, M., Feliu-Batlle, V., Benlahbib, B., Boukhetala, D. and Boudjema, F. (2021) Fuzzy Logic Controller-Based Maximum Power Point Tracking and Its Optimal Tuning in Photovoltaic Systems. *Serbian Journal of Electrical Engineering*, **18**, 351-384. https://doi.org/10.2298/SJEE2103351B

[8] Abbas, A. (2025) Power Tracking and Performance Analysis of Hybrid Perturb-Observe, Particle Swarm Optimization and Fuzzy Logic-Based Improved MPPT Control

for Standalone PV System. *Technologies*, **13**, Article 112. https://doi.org/10.3390/technologies13030112

[9] Elgendy, M.A., Zahawi, B. and Atkinson, D.J. (2012) Assessment of Perturb and Observe MPPT Algorithm Implementation Techniques for PV Pumping Applications. *IEEE Transactions on Sustainable Energy*, **3**, 21-33. https://doi.org/10.1109/tste.2011.2168245

[10] Koutroulis, E., Kalaitzakis, K. and Voulgaris, N.C. (2001) Development of a Microcontroller-Based, Photovoltaic Maximum Power Point Tracking Control System. *IEEE Transactions on Power Electronics*, **16**, 46-54. https://doi.org/10.1109/63.903988

[11] Bouksaim, M., Mekhfioui, M. and Srifi, M.N. (2021) Design and Implementation of Modified INC, Conventional INC, and Fuzzy Logic Controllers Applied to a PV System under Variable Weather Conditions. *Designs*, **5**, Article 71. https://doi.org/10.3390/designs5040071

[12] Derbeli, M., Tahar, H., Bouzid, A. and Bacha, S. (2023) Fuzzy Logic MPPT Control of Photovoltaic System with Real-Time Implementation and Performance Evaluation. *Energies*, **16**, Article 748. https://doi.org/10.3390/en16020748

[13] Priyadarshi, N., Padmanaban, S., Holm-Nielsen, J. B., Blaabjerg, F. and Bhaskar, M. S. (2020) An Experimental Estimation of Hybrid ANFIS-PSO-Based MPPT for PV Grid Integration under Fluctuating Sun Irradiance. *IEEE Systems Journal*, **14**, 1218-1229. https://doi.org/10.1109/JSYST.2019.2949083

[14] Zadeh, L.A. (1973) Outline of a New Approach to the Analysis of Complex Systems and Decision Processes. *IEEE Transactions on Systems, Man, and Cybernetics*, **3**, 28-44. https://doi.org/10.1109/tsmc.1973.5408575

[15] Babajide, T., Yusuf, K. and Rajendran, R. (2021) Hybrid and Conventional MPPT Performance Comparison under Partial Shading Using PSO-FLC-INC Methods. *Renewable Energy Focus*, **37**, 79-89.

Appendix

Figure A1. Single Diode PV Model.
https://drive.google.com/file/d/1C_qEOzmm73FfNKbB9Bu-LIHtVr8EFJOXY/view?usp=drivesdk

Figure A2. (a) Block diagram of a standalone PV system. (b) Flow diagram of an MPPT controller.
https://drive.google.com/file/d/1QxJdeIW1lZnSt1T868lWd3zWg74Daa0F/view?usp=drivesdk

Figure A3. Flowchart for the P&O MPPT control algorithm.
https://drive.google.com/file/d/1kEuWremUaneNctRG-mFBUGEcxW5QTqNnM/view?usp=drivesdk

Figure A4. PSO algorithm flowchart.
https://drive.google.com/file/d/1Mh6dIQVErF5zz7Lx_dVj3b6gbAVOOfIO/view?usp=drivesdk